Concentration-Dependent Front Velocity of the Autocatalytic Hydrogenase Reaction

Gabriella Bodó,[†] Rui M. M. Branca,[†] Ágota Tóth,[‡] Dezsó Horváth,[‡] and Csaba Bagyinka[†*]
[†]Institute of Biophysics, Biological Research Center, Szeged, H-6726, Hungary; and [‡]Department of Physical Chemistry, University of Szeged, Szeged, H-6720, Hungary

ABSTRACT HynSL hydrogenase from *Thiocapsa roseopersicina* was applied to catalyze the oxidation of molecular hydrogen in a new, improved, thin-layer reaction chamber. Investigation of the nature of this catalysis via the development of reduced benzyl viologen showed clearly the typical characteristics of an autocatalytic reaction: propagation of a reaction front originating from a single point, with a constant velocity of front propagation. The dependence of the reaction velocity on enzyme concentration was a power function with a positive enzyme concentration threshold, with an exponent of 0.4 ± 0.05. This indicates that the autocatalyst is an enzyme form. The front velocity decreased on increase of the electron acceptor concentration, as a sign that the autocatalyst interacts directly with the final electron acceptor. Overall, it may be concluded that the autocatalyst is an enzyme form in which $[FeS]_{distal}$ is reduced. Model calculations corroborate this. Because the reduction of all [FeS] clusters would be possible in a nonautocatalytic reaction, we hypothesize a small conformational change in the enzyme, catalyzed by the autocatalyst, which removes a block in the electron flow in either [NiFe] → $[FeS]_{proximal}$ or the $[FeS]_{proximal}$ → $[FeS]_{distal}$ reaction step, or removes a block of the penetration of gaseous hydrogen from the surface to the [NiFe] cluster.

INTRODUCTION

Hydrogenases are metalloenzymes that catalyze the reversible oxidation of molecular hydrogen, $H_2 \rightleftharpoons 2p^+ + 2e^-$. Hydrogenases are present mostly in prokaryotes, but can also be found in some eukaryotes (1–4). [NiFe] hydrogenases consist of a small (~34 kDa) and a large subunit (~64 kDa); the large subunit incorporates the [NiFe] active center, which is presumed to bind and split the hydrogen molecule, whereas the small subunit contains two or three [FeS] clusters, which transport the electrons from the [NiFe] center to the terminal electron acceptor. The large subunit also contains a hydrogen channel; through which gaseous hydrogen penetrate into the middle of the protein, where the hydrogen-splitting [NiFe] active center is located (5).

The membrane-bound [NiFe] hydrogenase from the purple photosynthetic bacterium *Thiocapsa roseopersicina* (HynSL) exhibits high stability against oxygen, heat, and proteolytic digestion, properties that hydrogenases in general do not have (6–8). A number of enzyme forms have been distinguished by spectroscopic methods (9). Different conformers have also been identified by two-dimensional, SDS-SDS (sodium-dodecyl-sulfate) gel-electrophoresis (7,8).

We showed recently that the hydrogenase-catalyzed oxidation of hydrogen includes at least one autocatalytic step (10–12). This finding was based on the special patterns of the hydrogen-oxidation reaction in a thin-layer reaction chamber; on the autocatalytic oscillations in the fast absorption kinetics of the reduced methyl viologen-initiated reaction of hydrogenase, and on the special and long lag phase observed in the hydrogen-oxidation experiments. The question remains however, of the nature of this autocatalyst and, if it is an enzyme form as suggested previously, whether it can be identified as a previously spectroscopically characterized enzyme form.

Investigation of the reaction in a thin layer allows the determination of the velocity of the reaction front. The front can readily be identified via the intense color of reduced methyl or benzyl viologen. To examine the nature of the autocatalyst, we have now determined the dependence of the front velocity on the enzyme and substrate (benzyl viologen) concentrations.

To attempt to interpret the experimental findings, various autocatalytic models have been considered and evaluated, assuming a special form of the enzyme or of the reduced substrate as autocatalyst, and also different reaction orders. A comparison of the results of kinetic calculations and the experiments in a thin layer suggested the possibility that a special form of the enzyme interacts with the unactivated enzyme forms to facilitate the reaction, i.e., the autocatalyst is an enzyme form. An effort was made to pinpoint the exact location of the autocatalytic step in the enzyme cycle.

There are several autocatalytic enzyme reactions known. In the peroxidase system, the reaction mechanism contains autocatalysis, the enzyme merely catalyses some reaction steps (13). In auto-phosphorylation the enzyme is only the substrate of its active form (14). Furthermore, several allosteric enzyme reactions exist where the enzyme is simply activated/inhibited by its substrate or product (15). In our system hydrogenase presents a unique form of autocatalysis where the active enzyme form activates the inactive one, providing a scheme very similar to the prion reactions (16,17) and significantly different from known autocatalytic enzyme reactions.

Submitted November 16, 2008, and accepted for publication March 17, 2009.

*Correspondence: csaba@nucleus.szbk.u-szeged.hu

Editor: Patrick Loria.

0006-3495/09/06/4976/8 $2.00

doi: 10.1016/j.bpj.2009.03.024

MATERIALS AND METHODS

Purification of hydrogenase

The stable [NiFe] hydrogenase from *T. roseopersicina* (HynSL) (6–8) was purified as described previously (10). Both partially (before preparative gel electrophoresis) and fully purified enzymes were used for measurements, with no apparent difference in the results.

Thin-layer experiments

For thin-layer experiments, we constructed a special reaction chamber (Fig. 1 *A*), comprising a glass plate into which a cylindrical pit, 0.4 mm deep, and 36 mm in diameter was polished. Addition of reaction mixture (410 μl) into the pit resulted in a uniform, plane parallel, 0.4 mm thick reaction layer. The advantages of this arrangement are that the side-effects due to different layer thicknesses are not present; the reaction chamber can be illuminated from below. The reaction chamber was placed into a small anaerobic box with Plexiglas windows at the top and bottom (Fig. 1 *B*), with a septum in the top window. The chamber was flushed continuously with gaseous hydrogen; the surplus of hydrogen was released through a thin needle in the septum at the top of the anaerobic box. The septum also allowed the introduction of different ingredients into the reaction mixture.

The reaction mixture contained HynSL hydrogenase in concentration up to ~1000 nM in 20 mM Na-phosphate buffer of pH 7.0, and benzyl viologen (Sigma, St. Louis, MO) as artificial electron acceptor at different concentrations.

The reaction was illuminated by a commercial fluorescent light bulb (Tungsram, Hungary) usually used in the household, from below. A 10-cm layer of water in glass container as heat filter was applied between the lamp and the reaction mixture. The reaction was carried out at room temperature of 24°C.

A Sony DCR-PC350E digital camera was used to record the reaction at a rate of one frame per second. Recording started after the Plexiglas anaerobic box was closed, but before the initial air atmosphere was replaced.

Several reaction starting protocols were tried. The reaction was started either by flushing the box with gaseous hydrogen, or by flushing the box first with gaseous nitrogen and then with gaseous hydrogen, or first evacuating the box and then flushing it with gaseous hydrogen. The different starting procedure did not result in any obvious differences in reaction characteristics. Although the evacuation procedure allowed the most precise identification of the starting time, the resulting reduced pressure often caused boiling of the reaction mixture and, because the reaction layer was very thin, drops of fluid bubbled out from the pit. Accordingly, we used the simple hydrogen flushing procedure most frequently. This did not permit precise determination of the time of appearance of the first spot, so the exact lag time could not be determined.

Thin-layer experiments in a gel phase

In this special case, the reaction mixture was prepared in a 1-mm thick, 1.6% agarose gel, which was placed on a plastic grid. The other conditions of the experiment were the same as for the normal thin-layer experiments.

Determination of the front velocity

For determination of the front velocity we developed a program in MATLAB (The MathWorks, Natick, MA). In each reaction in the thin-layer experiments six different blue spots were selected (Fig. 2 *A*) and their radii were determined in each recorded picture frame. Because the frames were taken at 1 s intervals, the rate of increase of the radius could easily be determined, which furnished the front velocity of the individual spot. The front velocities of the six individual spots were averaged and the error was calculated.

Model calculations

Differential equations and partial differential equations were solved either with the CVODE program package, or with MATLAB programs (18).

RESULTS

Characterization of the reaction in thin-layer experiments

The rate of growth of the reduced benzyl viologen spots in the thin-layer reaction mixtures in the newly developed reaction chamber shows the special spatial pattern characteristic of an autocatalytic reaction. At every enzyme and electron acceptor concentrations, the reaction starts from distinct points (Fig. 2 *A*) that expand continuously until the whole mixture becomes blue. New blue spots appear and grow during the reaction. It is difficult to follow the spot velocities for prolonged periods because new spots develop nearby those that are being observed, and the spots eventually collide and fuse; thus, any particular individual spot exists for only a limited period of time. Hence we could not follow each spot for the same length of time, although each chosen spot existed for sufficiently long to allow determination the front velocity.

The spots grew at constant velocity throughout the experiment (Fig. 3) within experimental error. The six different spots always exhibited the same front velocity.

In some cases, an overall faint background blue color of reduced benzyl viologen appeared over a large area of the reaction chamber, gradually intensified and spread out. This was more frequent at high enzyme concentrations and also, if the chamber was not cleaned sufficiently carefully. Both mechanical cleaning (brushing) and washing with a detergent decreased the probability of this background coloring.

It should be mentioned that in most, but not in all experiments, reaction spots also readily started at the edges of the

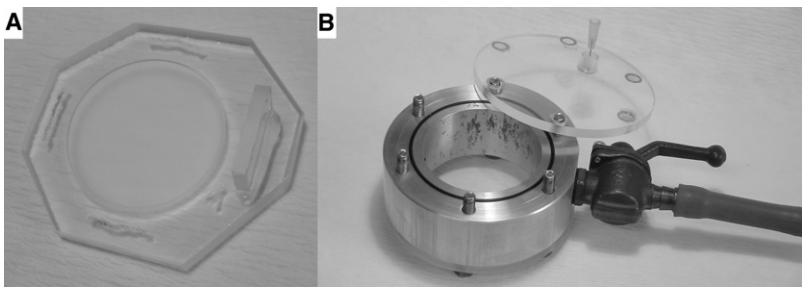

FIGURE 1 (*A*) Reaction chamber and (*B*) anaerobic box.

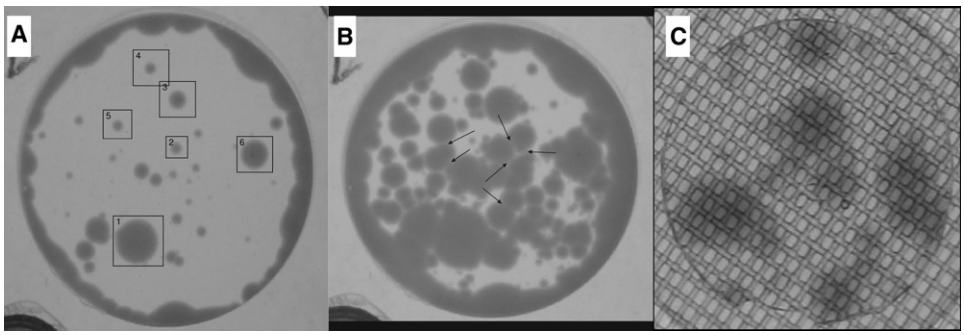

FIGURE 2 Pattern of hydrogen-oxidation reaction in thin-layer experiments. (*A*) Six spots were selected for determination of the front velocity. (*B*) Collision of the fronts. Arrows mark the white demarcation areas. (*C*) Thin-layer experiment carried out in agarose gel. The electron acceptor concentration at each measurement was 2 mM.

pit likewise growing in time. Nevertheless, in these cases too individual spots appeared in the middle of the reaction chamber, and such spots were chosen for determination of the front velocity.

When two spots met, a white line could be observed at the interface of the two fronts, which separated the two circles even when the apparent overlap of the two circles was quite appreciable (Fig. 2 *B*). As the reaction proceeded, however, this white demarcation line disappeared.

At the end of the reaction, the total reaction volume was blue, but the final optical density of the reaction mixture depended on the enzyme concentration, which is not characteristic for an enzyme reaction at all. Because our technique does not allow precise determination of the final optical density of the reduced benzyl viologen in the reaction chamber, quantitative data are not available. It was obvious from visual observation, however, that the final color of the reaction was fainter at lower enzyme concentrations, although the initial benzyl viologen concentration was the same in each case.

When the reaction was carried out in 1.6% agarose gel, the reaction pattern was very much the same as in solution (Fig. 2 *C*). Blue spots appeared and expanded in time and at the end of the reaction the whole gel was blue. Nevertheless, it was more difficult to determine of the front, because the grid holding the gel disturbed the visualization.

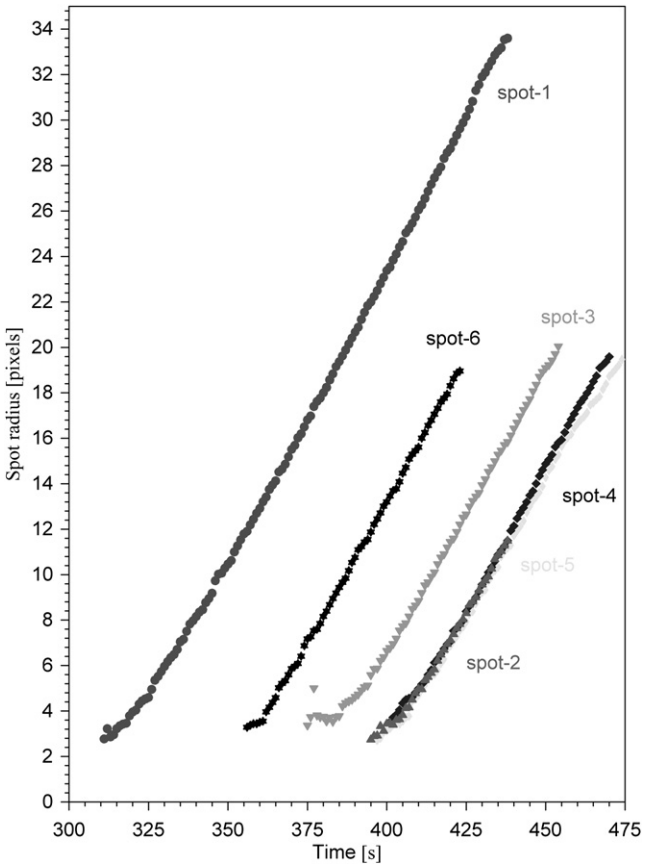

FIGURE 3 Front velocity of different spots in a thin-layer experiment (same experiment as in Fig. 2 *A*). Spots 2, 4, and 5 overlap.

Concentration dependence of the front velocity

We carried out two series of measurements of the dependence of the front velocity on the enzyme concentration (Fig. 4 *A*). The first series yielded only three points (*squares*) in steps in which the concentration was halved. In the second series (*circles*), the starting concentration was the same, but eight additional point were obtained by stepwise reduction of the concentrations by one-third.

As anticipated, the front velocity increased by increasing enzyme concentrations, though not linearly (Fig. 4 *A*). Fitting a power function to all the data points yielded a power of 0.4 $\pm$ 0.05; it is striking that the power function crossed the x (protein concentration) axis at a positive protein concentration, estimated to be 18 nM. The front velocity of the spots in 1.6% agarose gel, included in Fig. 4 *A* (*open square*), fits the curve well, as an indication that the diffusion is not limited by the gel matrix.

It was surprising, however, that the front velocity decreased on increase of the electron acceptor (benzyl viologen) concentration (Fig. 5 *A*) at all measured hydrogenase concentrations.

Model calculations

For model calculations, the autocatalytic model defined previously (12) was modified, but the key features of the activation process and the autocatalytic step were preserved.

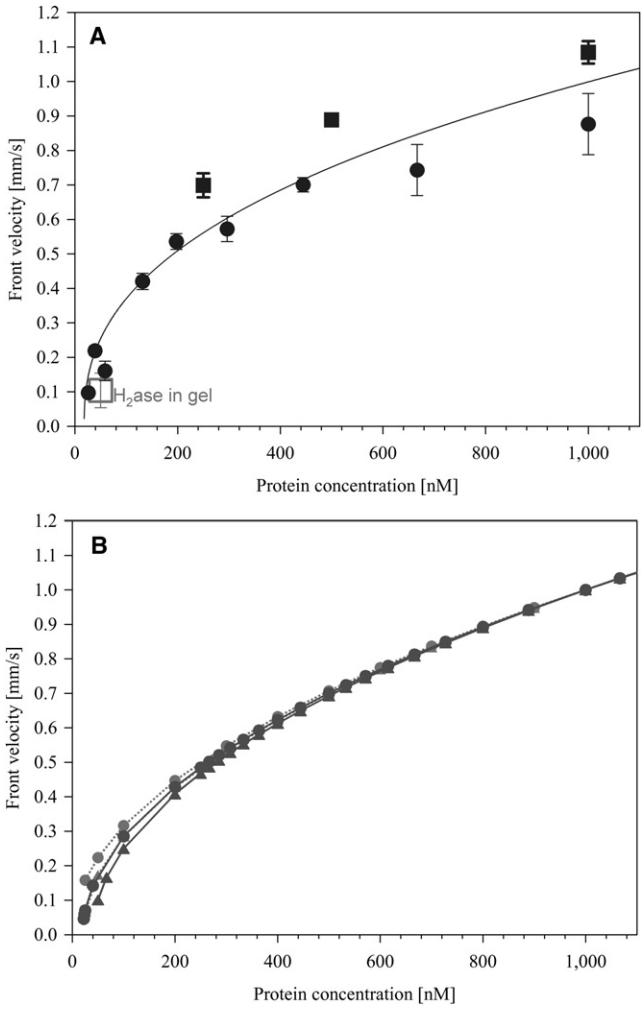

FIGURE 4 Dependence of front velocities on enzyme concentration. (*A*) Data from two parallel experiments. (*B*) Model fittings (*solid line*, Model 1; *dotted line*, Model 2).

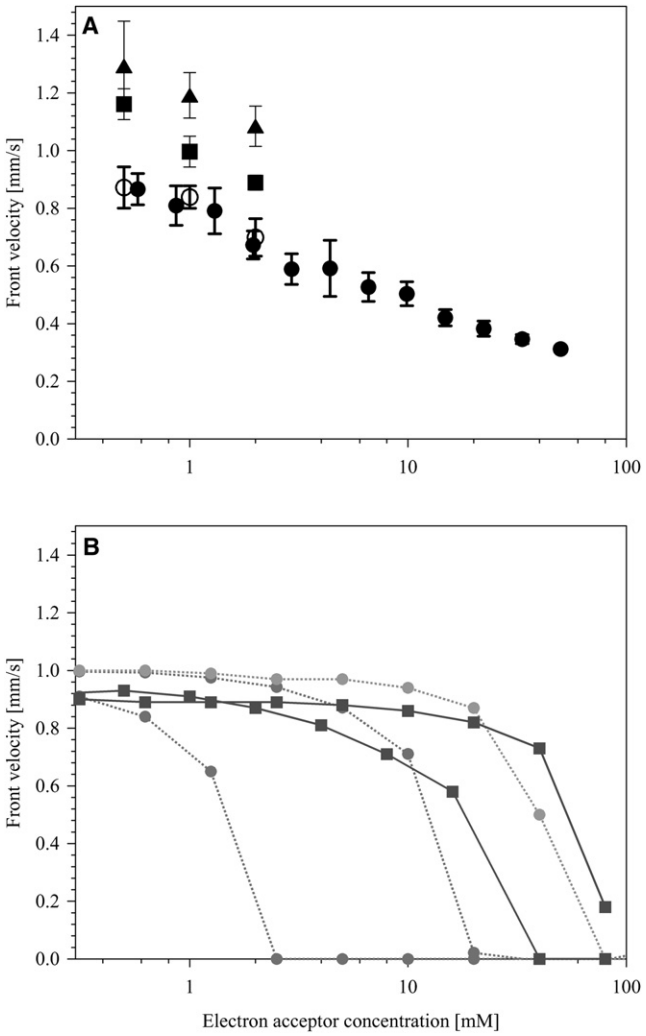

FIGURE 5 Dependence of front velocities on electron acceptor concentration. (*A*) Experimental data at three different enzyme concentrations (▲, 1000 nM; ■, 500 nM; ○, 250 nM). (*B*) Model fittings (●, Model 1; ■, Model 2).

For construction of the simplest feasible model system, the two important new, to our knowledge, experimental observations presented above were focused on:

- The velocity of front propagation is approximately proportional to the square root of the total enzyme concentration.
- The velocity of front propagation decreases with increasing electron-acceptor concentration.

The first observation implies that the autocatalytic step is a second-order reaction with respect to the kinetics (19), whereas the second observation requires that the substrate reacts directly with the autocatalyst form of the enzyme (20,21). These observations impose slight modifications on the previous model (12).

In the experiments, the reaction chamber was flushed with gaseous hydrogen, and the hydrogen concentration was therefore constant throughout the experiment. Accordingly, we did not include any hydrogen binding step in the model, which would merely have scaled the rate constant of the corresponding reaction. It should be mentioned, however, that during the enzyme cycle the oxidation state of the enzyme should be re-established, and therefore at least three different enzyme forms must be included in the enzyme cycle.

Two generic models are presented in this study from among the several that have been constructed: one considers the autocatalytic conversion of E_2 into E_3 within the enzymatic cycle (Model 1), in the other it is outside the enzyme cycle, although the autocatalyst remains inside the enzyme cycle (Model 2).

Model 1: autocatalysis within the cycle

In a distributed system, the governing equations for Model 1 are

$$
\begin{aligned}
\partial[E_1]/\partial t &= D_1\,\nabla^2[E_1] - k_{1f}[E_1]\\
\partial[E_2]/\partial t &= D_2\,\nabla^2[E_2] + k_{1f}[E_1] - k_{2a}[E_2][E_3] - k_{2f}[E_2] + k_{2b}[E_3] + k_{cf}[E_4][M_o]\\
\partial[E_3]/\partial t &= D_3\,\nabla^2[E_3] + k_{2a}[E_2][E_3] + k_{2f}[E_2] - k_{2b}[E_3] - k_{3f}[E_3][M_o]\\
\partial[E_4]/\partial t &= D_4\,\nabla^2[E_4] + k_{3f}[E_3][M_o] - k_{cf}[E_4][M_o]\\
\partial[M_o]/\partial t &= D_o\,\nabla^2[M_o] - k_{3f}[E_3][M_o] - k_{cf}[E_4][M_o]\\
\partial[M_r]/\partial t &= D_r\,\nabla^2[M_r] + k_{3f}[E_3][M_r] + k_{cf}[E_4][M_r],
\end{aligned}
\tag{1}
$$

where the variables E_i are the different enzyme forms, whereas M_o and M_r are the oxidized and reduced forms of the electron acceptor, and $[M_o] + [M_r] = \text{constant}$. The front velocity of M_r formation can be measured experimentally. Without loss of generality, we may consider one spatial dimension (because it is obvious from the experiments that a single reaction is axial symmetric) and introduce dimensionless variables. The different enzyme forms have the same diffusion rate ($D_1 = D_2 = D_3 = D_4$). Benzyl viologen may diffuse slightly faster but its two forms have the same diffusion constant ($D_o = D_r$). The concentration of the substrate, however, is much greater than that of the enzyme therefore has a negligible gradient at the reaction front. Hence we may use a single diffusion coefficient for all species, because the diffusion of the substrate has only a minor contribution to the velocity of propagation, which is governed mainly by the diffusion of the various forms of the enzyme.

Because the diffusion constants have been set the same, the length scales as $\xi = (k_{2a}E_T/D)^{1/2}x$. The time ($t$) is transformed to $\tau = k_{2a}E_Tt$. The concentrations are scaled to the total amount of enzyme (E_T): $e_i = [E_i]/E_T$, $m_o = [M_o]/E_T$, $m_r = [M_r]/E_T$. This yields

$$
\begin{aligned}
\partial e_1/\partial\tau &= \partial^2 e_1/\partial\xi^2 - \kappa_{1f}\,e_1\\
\partial e_2/\partial\tau &= \partial^2 e_2/\partial\xi^2 + \kappa_{1f}\,e_1 - e_2\,e_3 - \kappa_{2f}\,e_2 + \kappa_{2b}\,e_3\\
&\quad + \kappa_{cf}\,e_4\,m_o\\
\partial e_3/\partial\tau &= \partial^2 e_3/\partial\xi^2 + e_2\,e_3 + \kappa_{2f}\,e_2 - \kappa_{2b}\,e_3 - \kappa_{3f}\,e_3\,m_o\\
\partial e_4/\partial\tau &= \partial^2 e_4/\partial\xi^2 + \kappa_{3f}\,e_3\,m_o - \kappa_{cf}\,e_4\,m_o\\
\partial m_o/\partial\tau &= \partial^2 m_o/\partial\xi^2 - \kappa_{3f}\,e_3\,m_o - \kappa_{cf}\,e_4\,m_o\\
\partial m_r/\partial\tau &= \partial^2 m_r/\partial\xi^2 + \kappa_{3f}\,e_3\,m_o + \kappa_{cf}\,e_4\,m_o,
\end{aligned}
\tag{2}
$$

where $\kappa_i = k_i/(k_{2a}\,E_T)$ for each first-order kinetic constant (κ_{1f}, κ_{2f}, κ_{2b}) and $\kappa_i = k_i/k_{2a}$ for each second-order kinetic constant (κ_{3f}, κ_{cf}).

To facilitate the calculations we made several simplifications. We are interested in the front velocity of the reaction, and therefore the slow production of E_2 from E_1 was neglected, and the κ_{1f} rate constant was set to zero. Because the experimental findings indicate that the nonautocatalytic bulk reaction $E_2 \rightarrow E_3$ is very slow and does not affect the front velocity, κ_{2f} was also set to zero.

On the autocatalysis timescale, the decrease in the concentration of M_o is at most of the same order as the concentration of E_3 produced, and therefore the concentration of M_o is essentially constant in the vicinity of the reaction front. In this case, the reverse step $E_2 \leftarrow E_3$ cannot be distinguished from the path $E_3 \rightarrow E_4 \rightarrow E_2$, and therefore κ_{2b} was also set to zero.

The value of κ_{3f} was adjusted so that, at constant substrate concentration, the extinction of the reaction fronts occurs at an enzyme concentration comparable to that observed experimentally.

The initial conditions of the reaction at $\tau = 0$ with grid spacing 0.1 and no-flux boundary conditions: in the spatial region [0,10] were $E_2 = (1 - p)E_T$, $E_3 = pE_T$; all other enzyme components were set to zero; in the spatial region [10,1000], $E_2 = E_T$, and all other enzyme components were zero. The parameter p was varied in the interval 0.001–1, although it did not significantly affect the front velocity.

The dependence of the front velocity on enzyme concentration for this model with two different parameter sets is presented in Fig. 4 *B* (*solid lines*), whereas the dependence on the electron acceptor concentration at three different enzyme concentrations is presented in Fig. 5 *B* (*circles*).

Model 2: autocatalysis outside the cycle

In a distributed system, the governing equations for the constructed model are

$$
\begin{aligned}
\partial[E_1]/\partial t &= D_1\,\nabla^2[E_1] - k_{1f}[E_1]\\
\partial[E_2]/\partial t &= D_2\,\nabla^2[E_2] + k_{1f}[E_1] - k_{2a}[E_2][E_3] - k_{2f}[E_2] + k_{2b}[E_3]\\
\partial[E_3]/\partial t &= D_3\,\nabla^2[E_3] + k_{2a}[E_2][E_3] + k_{2f}[E_2] - k_{2b}[E_3] - k_{3f}[E_3][M_o] + k_{cf}[E_5]\\
\partial[E_4]/\partial t &= D_4\,\nabla^2[E_4] + k_{3f}[E_3][M_o] - k_{4f}[E_4][M_o]\\
\partial[E_5]/\partial t &= D_5\,\nabla^2[E_5] + k_{4f}[E_4][M_o] - k_{cf}[E_5]\\
\partial[M_o]/\partial t &= D_o\,\nabla^2[M_o] - k_{3f}[E_3][M_o] - k_{4f}[E_4][M_o]\\
\partial[M_r]/\partial t &= D_r\,\nabla^2[M_r] + k_{3f}[E_3][M_r] + k_{4f}[E_4][M_r].
\end{aligned}
\tag{3}
$$

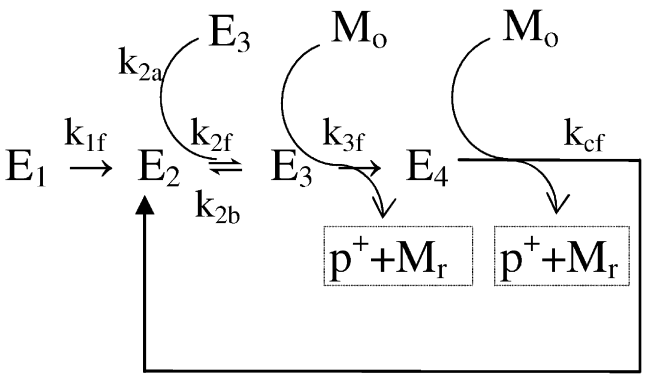

FIGURE 6 Model 1. Modified triangular model that considers the autocatalytic conversion of E_2 into E_3 within the enzymatic cycle.

The same transformations as for Eq. 1 yield:

$$\begin{aligned}
\partial e_1/\partial\tau &= \partial^2 e_1/\partial\xi^2 - \kappa_{1f}\, e_1\\
\partial e_2/\partial\tau &= \partial^2 e_2/\partial\xi^2 + \kappa_{1f}\, e_1 - e_2\, e_3 - \kappa_{2f}\, e_2 + \kappa_{2b}\, e_3\\
\partial e_3/\partial\tau &= \partial^2 e_3/\partial\xi^2 + e_2\, e_3 + \kappa_{2f}\, e_2 - \kappa_{2b}\, e_3\\
&\quad -\kappa_{3f}\, e_3\, m_o + \kappa_{cf}\, e_5\\
\partial e_4/\partial\tau &= \partial^2 e_4/\partial\xi^2 + \kappa_{3f}\, e_3\, m_o - \kappa_{4f}\, e_4\, m_o\\
\partial e_5/\partial\tau &= \partial^2 e_5/\partial\xi^2 + \kappa_{4f}\, e_4\, m_o - \kappa_{cf}\, e_5\\
\partial m_o/\partial\tau &= \partial^2 m_o/\partial\xi^2 - \kappa_{3f}\, e_3\, m_o - \kappa_{4f}\, e_4\, m_o\\
\partial m_r/\partial\tau &= \partial^2 m_r/\partial\xi^2 + \kappa_{3f}\, e_3\, m_o + \kappa_{4f}\, e_4\, m_o.
\end{aligned} \tag{4}$$

During the calculations, the contributions of the production of E_2 ($E_1 \rightarrow E_2$) and the noncatalyzed conversion of E_2 to E_3 ($E_2 \rightarrow E_3$) were neglected in the same way as in the first model ($\kappa_{1f} = 0$ and $\kappa_{2f} = 0$).

With the autocatalysis outside the cycle, it is not the rate constant of the consumption of the autocatalyst E_3 (κ_{3f}) that determines the concentration of E_3, but the ratio of the rates in the cycle. This allows the fast reduction of the substrate behind the autocatalytic front that is not possible in Model 1. The fast cycle behind the autocatalytic step itself does not lead to the extinction of the reaction front because it resembles the reversible removal of the autocatalyst (21); we

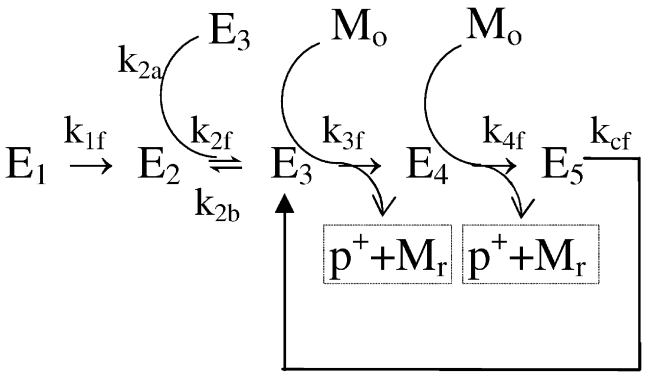

FIGURE 7 Model 2. Modified triangular model that considers the autocatalytic conversion of E_2 into E_3 in the outside the enzyme cycle, although the autocatalyst remains inside the enzyme cycle.

therefore included the reverse step $E_2 \leftarrow E_3$ ($\kappa_{2b} \neq 0$). The rate constants were again adjusted so that the front extinction corresponded to the experimentally observed magnitude. The initial conditions were the same as for Model 1.

It should be mentioned that in this model there must be two different hydrogen-binding reactions, one inside the enzyme cycle and another one outside it.

The dependence of the front velocity on enzyme concentration for this model with two different parameter sets is presented in Fig. 4 *B* (*dotted lines*), whereas the dependence on the electron acceptor concentration at three different enzyme concentrations is presented in Fig. 5 *B* (*squares*).

DISCUSSION

We earlier suggested that an autocatalytic reaction occurs during the hydrogen oxidation reaction (10–12). The constant velocity of the reaction front, and the separate reaction centers are all specific for such reactions, and have been investigated previously. The suggestion was also supported by seeding the front either with a small drop of ''activated'' enzyme or with a high concentration of reduced benzyl viologen (a low concentration of reduced benzyl viologen could not seed the reaction front). The reaction in the new thin-layer chamber displays all of these characteristics of the autocatalytic reaction, but in this study they are even clearer and more pronounced. We have carried out additional experiments and have further evidence to support the suggestion.

The conclusion of the existence of this autocatalytic reaction holds true only if the reaction mixture is homogeneous. There is no question about the homogeneous distribution of the electron acceptor (benzyl viologen) in the reaction chamber because it is a water-soluble compound. Hydrogenase is also water-soluble, though some aggregation can not be ruled out because HynSL from *T. roseopersicina* is located in the membrane (22–25). If only unevenly present, aggregated hydrogenase catalyzes the reaction, the spots would be present in consequence of the uneven distribution of the hydrogenase in the reaction chamber. In the middle of every spot, there would be an aggregated hydrogenase seed catalyzing the reaction, in which case the reaction would occur only at a single point (where the hydrogenase is active, its diffusion being negligible because of the size of the aggregate) consequently the rate of the growth of the spots would be determined solely by the diffusion of the substrate in the solution (the oxidized form of the substrate must diffuse into the middle of the spot, where all the oxidized form has already been used up, and the reduced substrate must diffuse out from the center). It is evident that this would cause a decreasing front velocity in time (larger spots expanding more slowly), which is obviously not the case. At all measured enzyme and electron acceptor (benzyl viologen) concentrations, a linear front evolution and thus a constant front velocity was observed (Fig. 3) throughout the timescale investigated.

Another possibility is uneven distribution of the gaseous hydrogen. Although it is true that at the start of the reaction the atmosphere in the reaction chamber is air and the hydrogen slowly displaces it, this explanation can be ruled out, because the same reaction pattern was observed when we first evacuated the reaction chamber and then filled it with hydrogen. Another argument is that the time for diffusion through the layer is only 16 s, a time too short when compared to any of the important reaction timescales observed in these experiments (the diffusion coefficient of hydrogen in water is 5×10^{-5} cm^2/s (26)).

It is likewise not possible that the hydrogen penetration into the solution is uneven. This would mean that there are channels through the surface where the hydrogen enters the solution, and the spots are due to the diffusion of the hydrogen through these channels. First, there is no reason to hypothesize the existence of such channels, and again it results in a nonlinear front velocity in time. Moreover, when the reaction was carried out in flasks and the reaction mixture was vigorously shaken before the reaction started, so that there was no doubt about the hydrogen penetrating into the solution, this pattern was similarly observed.

We must mention that convection does not play any role in the thin-layer experiments because growing spots were also observed with no significant change in front velocity (Fig. 4 *A*, *open square*) when the reaction mixture was incorporated into a 1.6% agarose gel (Fig. 2 *C*), where convection was blocked and only diffusion was allowed.

Because all the reaction components are homogeneous it may be concluded that the observed reaction pattern is not an artifact, i.e., autocatalytic fronts do arise.

The questions remain of the nature of the autocatalyst and when the autocatalytic step takes place. In an earlier study, we proposed and investigated a very much similar model (12) that gave a reasonable description of the observed characteristics of the autocatalytic reaction (the activation of the enzyme, the lag phase of the activation and of the reaction, the concentration limit for the inactivated enzyme, etc.) in a batch reactor. We have analyzed the model thoroughly, as well as the dependence on the characteristic and experimentally observable model parameters (12). We concluded that the autocatalyst is an enzyme form located in the enzyme cycle. In view of our new, to our knowledge, experimental findings, we can improve the model by including spatial distribution of the components and setting the autocatalyst as an electron donor form of the enzyme.

With the use of the modified models in which the autocatalytic step is situated inside (Fig. 6) or outside (Fig. 7) the enzymatic cycle, we carried out in silico experiments and theoretical calculations to simulate the real experiments in the thin-layer reaction chamber.

The experiments showed that, at least in a certain concentration range, the front velocity decreases with increasing electron acceptor concentration (Fig. 5 *A*). This finding allows us to rule out the reduced electron acceptor as an autocatalyst. If a trace amount of reduced electron acceptor present in the benzyl viologen solution were the autocatalyst, an increase of the overall concentration of the electron acceptor would simultaneously increase the autocatalyst concentration and this would increase the front velocity. Because this was not the case (Fig. 5 *A*), we can definitely rule out this possibility.

As discussed previously (10–12), there remains only a hydrogenase form as autocatalyst. The dependence of the front velocity on the enzyme concentration corroborates this possibility (Fig. 4). The front velocity increases as the overall enzyme concentration (and hence the concentration of the autocatalyst form of the enzyme) is increased. The relation can be described well as a power function of the enzyme concentration. The best fit calculated from several independent experiments, is given by as 0.4 ± 0.05. The threshold value (where the power function crosses the x axis, and below which the reaction never starts) is 18 nM. This is in accordance with the theoretical calculations on the earlier, simpler model (10–12) where we showed the existence of such a threshold enzyme concentration. This is only an upper limit for the threshold because the hydrogenase used in this experiment was not 100% pure, and we do not know the partial concentration of the autocatalyst in the protein.

In the in silico experiments, both models indicated a square root dependence of the front velocity on the enzyme concentration. The front velocity observed in real-life experiment was slightly less than this, so some other reactions should also influence the front velocity. Similarly to the earlier, simpler model, the model calculation also foresees the experimentally observed concentration barrier below which the reaction does not start. It was possible to simulate the background reaction, when the whole reaction chamber becomes blue without spot formation, by setting the nonautocatalytic rate constant to a nonzero value. These findings strengthen the suggestion that the autocatalyst is some hydrogenase form. However, from this dependence alone it is not possible to locate the place of the autocatalytic step within the enzymatic reaction.

Nonetheless the dependence of the front velocity on the electron acceptor concentration permitted determination of the approximate location of the autocatalytic step. We found that, on increase of the overall electron acceptor concentration, the front velocity decreased (Fig. 5); consequently the autocatalyst concentration should decrease on increase of the electron acceptor concentration. This phenomenon can be achieved only if the oxidized electron acceptor interacts directly with the autocatalyst form of the enzyme. We can assume that the electron acceptor interacts only with the $[FeS]_{distal}$ cluster in the hydrogenase, and accordingly this experiment indicates that the autocatalyst is a hydrogenase form in which the $[FeS]_{distal}$ cluster holds an electron (i.e., at least the $[FeS]_{distal}$ cluster is reduced).

It has long been known that hydrogenase needs ''activation'' to achieve full activity. Such activation can be achieved by incubating the enzyme under hydrogen (9,27). Because the activation itself has a lag phase (27) and also

because the activated hydrogenase displays a lag phase in the hydrogen-oxidation reaction (10–12), we concluded that the autocatalytic step occurs after the enzyme binds the gaseous hydrogen, and that the autocatalytic step is situated inside the enzyme cycle. The in silico model experiments, however, did not provide definite support for this assumption. Both models can depict the decreasing front velocity on increasing electron acceptor concentration but with both models the transition from the full velocity to zero is sharper than what was measured experimentally (Fig. 5).

CONCLUSION

We have shown that hydrogenase during its reaction cycle has an autocatalytic step. The autocatalytic step can not be a simple reduction of the $[FeS]_{distal}$ cluster. Because the electron pathway for hydrogenase from *T. roseopersicina* (in which there are just two [FeS] clusters (28,29)) is [NiFe] $\rightarrow$ $[FeS]_{proximal}$ $\rightarrow$ $[FeS]_{distal}$ $\rightarrow$ [electron acceptor], reduction of the clusters is possible through normal enzyme reactions without any autocatalytic step. Because the autocatalytic step does take place, there should be either a block in the electron flow in the reaction steps [NiFe] $\rightarrow$ $[FeS]_{proximal}$ or $[FeS]_{proximal}$ $\rightarrow$ $[FeS]_{distal}$, or a block of gaseous hydrogen penetration from the surface to the [NiFe] cluster. This block is eliminated by the autocatalytic reaction. Any of these possibilities may involve a (possibly slight) conformational change in the protein.

We thank Rózsa Verebély for technical assistance.

This work was supported by the Hungarian Science Foundation (OTKA T049276, OTKA T049207), AUTOESKORT, the Portuguese Science and Technology Foundation, and the Operational Program for the Science, Technology and Innovation (PhD fellowship SFRH/BD/13128/2003 to R.M.M.B.).

REFERENCES

1. Volbeda, A., M. H. Charon, C. Piras, E. C. Hatchikian, M. Frey, et al. 1995. Crystal structure of the nickel-iron hydrogenase from *Desulfovibrio gigas*. *Nature*. 373:580–587.
2. Armstrong, F. A. 2004. Hydrogenases: active site puzzles and progress. *Curr. Opin. Chem. Biol.* 8:133–140.
3. Albracht, S. P. J. 2001. Spectroscopy: the functional puzzle. *In* Hydrogen as a Fuel: Learning From Nature. R. Cammack, M. Frey, and R. Robson, editors. Taylor and Francis, UK/NY, London, New York. 110–158.
4. Cammack, R. 2001. Hydrogenases and their activities. *In* Hydrogen as a Fuel: Learning From Nature. R. Cammack, M. Frey, and R. Robson, editors. Taylor and Francis, UK/NY, London, New York. 73–92.
5. Montet, Y., P. Amara, A. Volbeda, X. Verned, E. C. Hatchikian, et al. 1997. Gas access to the active site of Ni-Fe hydrogenases probed by X-ray crystallography and molecular dynamics. *Nat. Struct. Biol.* 4:523–526.
6. Bagyinka, C., Z. Dancsházy, K. L. Kovács, P. Ormos, and L. Keszthelyi. 1981. Studies on solar energy conversion by *Halobacteria* and *Thiocapsae*. *Acta Biol. Acad. Sc. Hung.* 32:311–325.
7. Kovács, K. L., and C. Bagyinka. 1990. Structural properties, functional states and physiological roles of hydrogenase in photosynthetic bacteria. *FEMS Microbiol. Rev.* 87:407–412.
8. Kovács, K. L., G. Tigyi, L. T. Thanh, S. Lakatos, Z. Kiss, et al. 1991. Structural rearrangements in active and inactive forms of hydrogenase from *Thiocapsa roseopersicina*. *J. Biol. Chem.* 266:947–951.
9. Cammack, R., C. Bagyinka, and K. L. Kovács. 1989. Spectroscopic characterization of the nickel and iron-sulphur clusters of hydrogenase from the purple photosynthetic bacterium *Thiocapsa roseopersicina*. 1. Electron spin resonance spectroscopy. *Eur. J. Biochem.* 182:357–362.
10. Bagyinka, C., J. Ősz, and S. Száraz. 2003. Autocatalytic oscillations in the early phase of the photoreduced methyl viologen-initiated fast kinetic reaction of hydrogenase. *J. Biol. Chem.* 278:20624–20627.
11. Ősz, J., and C. Bagyinka. 2005. An autocatalytic step in the reaction cycle of hydrogenase from *Thiocapsa roseopersicina* can explain the special characteristics of the enzyme reaction. *Biophys. J.* 89:1984–1989.
12. Ősz, J., G. Bodó, R. M. M. Branca, and C. Bagyinka. 2005. Theoretical calculations on hydrogenase kinetics: explanation of the lag phase and the enzyme concentration dependence of the activity of hydrogenase uptake. *Biophys. J.* 89:1957–1964.
13. Bronnikova, T. V., V. R. Fed'kina, W. M. Schaffer, and L. F. Olsen. 1995. Period-doubling bifurcations and chaos in a detailed model of the peroxidase-oxidase reaction. *J. Phys. Chem.* 99:9309–9312.
14. Adams, J. A. 2001. Kinetic and catalytic mechanisms of protein kinases. *Chem. Rev.* 101:2271–2290.
15. Garret, R. H., and C. M. Grisham. 1999. Biochemistry. Saunders College Publishing, Fort Worth.
16. Rössler, O. E., J. L. Hudson, R. Rössler, and J. Parisi. 1998. BSE viewed dynamically: a possible early cure based on passive immunization against PrP^{Sc}. *In* A Perspective Look at Nonlinear Media. Lecture Notes in Physics. Springer, Berlin, Heidelberg. 192–196.
17. Eigen, M. 1996. Prionics or the kinetic basis of prion diseases. *Biophys. Chem.* 63:A1–A18.
18. Cohen, S. D., and A. C. Hindmarsh. 1996. CVODE, a stiff/nonstiff ODE solver in C. *Comput. Phys.* 10:138–148.
19. Scott, S. K., and K. Showalter. 1992. Simple and complex propagating reaction-diffusion fronts. *J. Phys. Chem.* 96:8702–8711.
20. Tóth, Á., D. Horváth, É. Jakab, J. H. Merkin, and S. K. Scott. 2001. Lateral instabilities in cubic autocatalytic reaction fronts: the effect of autocatalyst decay. *J. Chem. Phys.* 114:9947–9952.
21. Jakab, É., D. Horváth, Á. Tóth, J. H. Merkin, and S. K. Scott. 2001. The effect of reversible binding of the autocatalyst on the lateral instability of reaction fronts. *Chem. Phys. Lett.* 342:317–322.
22. Kovács, K. L., C. Bagyinka, and L. T. Serebriakova. 1983. Distribution and orientation of hydrogenase in various photosynthetic bacteria. *Curr. Microbiol.* 9:215–218.
23. Bagyinka, C., K. L. Kovács, and E. Rák. 1982. Localization of hydrogenase in *Thiocapsa roseopersicina* photosynthetic membrane. *Biochem. J.* 202:255–258.
24. Bagyinka, C., A. Dér, and K. L. Kovács. 1983. Orientation of hydrogenase enzyme in various photosynthetic bacteria. *Acta Biochim. Biophys. Hung.* 18, 86–86.
25. Kovács, K. L., C. Bagyinka, and E. Rák. 1982. Orientation of hydrogenase in the photosynthetic membrane of *Thiocapsa roseopersicina*. *Stud. Biophys.* 90:71–72.
26. Ferrell, R. T., and D. M. Himmelblau. 1967. Diffusion coefficients of hydrogen and helium in water. *AIChE J.* 13:702–708.
27. Lissolo, T., S. Pulvin, and D. Thomas. 1984. Reactivation of the hydrogenase from *Desulfovibrio gigas* by hydrogen. Influence of redox potential. *J. Biol. Chem.* 259:11725–11729.
28. Bagyinka, C., J. P. Whitehead, and M. J. Maroney. 1993. An x-ray absorption spectroscopic study of nickel redox chemistry in hydrogenase. *J. Am. Chem. Soc.* 115:3576–3585.
29. Bagyinka, C., Z. Szőkefalvi-Nagy, I. Demeter, and K. L. Kovács. 1989. Metal composition analysis of hydrogenase from *Thiocapsa roseopersicina* by proton induced X-ray emission spectroscopy. *Biochem. Biophys. Res. Commun.* 162:422–426.